ACS Chemical Neuroscience

pubs.acs.org/chemneuro Letter

Influence of Lipid Membranes on α-Synuclein Aggregation

Andrii S. Kurochka, Dmytro A. Yushchenko, Petr Bouř, and Volodymyr V. Shvadchak*

Cite This: ACS Chem. Neurosci. 2021, 12, 825–830 Read Online

ACCESS | Metrics & More | Article Recommendations | Supporting Information

ABSTRACT: α-Synuclein is a neuronal protein involved in synaptic vesicle trafficking. During the course of Parkinson's disease, it aggregates, forming amyloid fibrils that accumulate in the midbrain. This pathological fibrillization process is strongly modulated by physiological interactions of α-synuclein with lipid membranes. However, the detailed mechanism of this effect remains unclear. In this work, we used environment-sensitive fluorescent dyes to study the influence of model lipid membranes on the kinetics of α-synuclein fibrillization. We observed that formation of the fibrils from α-synuclein monomers is strongly delayed even by small amounts of lipids. Furthermore, we found that membrane-bound α-synuclein monomers are not involved in fibril elongation. Hence, presence of lipids slows down fibril growth proportionally to the fraction of membrane-bound protein.

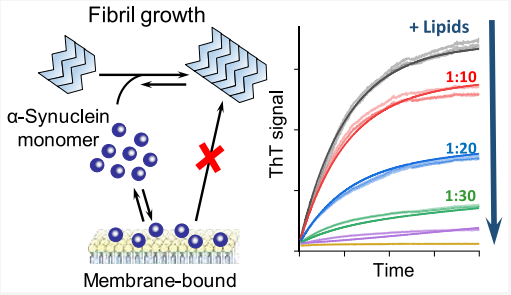

KEYWORDS: *amyloid, fibril, fibrillization, kinetics, lag time, liposomes*

α-Synuclein (αSyn) is a 140 amino acid protein which is predominantly localized in presynaptic terminals of neurons.[1] Physiological functions of αSyn are associated with synaptic vesicle trafficking and membrane fusion.[2,3] αSyn is intrinsically disordered in solution and adopts a helical conformation upon binding to membranes.[4]

During the course of Parkinson's disease, αSyn aggregates, forming amyloid fibrils that accumulate in the neurons as pathological inclusions called Lewy bodies.[5] These fibrils are up to several micrometers long and are composed of thousands of monomers. The monomers are ordered in parallel β-sheet conformation and connected by multiple hydrogen bonds.[6] αSyn fibrils were reported to be toxic for cell cultures[7] and to induce amyloid formation *in vivo*,[8] that points to prion-like nature of αSyn fibrillization. Specially designed αSyn mutants with hindered membrane binding exhibited significantly higher toxicity than wild type (WT) αSyn when expressed in transgenic cells or in mice.[9] Moreover, one of the mutations causing early onset of Parkinson's disease (A30P)[10] directly reduces αSyn affinity to the membrane while it does not affect the protein fibrillization core.[11]

αSyn fibrillization is a multistep process that can be described by a sigmoidal kinetic curve. It starts from the primary nucleation, a relatively slow assembly of unstructured monomers into the initial fibrils.[12] This assembly is believed to occur via oligomeric intermediates.[13] After formation, the first fibrils rapidly elongate by recruiting new αSyn monomers to the fibril ends,[14] until all monomer in the solution is converted to fibrillar form.

In cells, monomeric or oligomeric αSyn can bind to membranes affecting fibrillization. The influence of lipid membranes on αSyn aggregation was intensively studied *in vitro*.[15] However, the reported results from these studies are often contradictory (see literature overview in Table S1). For example, membranes composed of short chain anionic phosphatidylserine lipids were reported to induce αSyn aggregation at low lipid to protein ratios and to suppress it when present in large excess over αSyn.[16] On the other hand, vesicles composed of mixtures of negatively charged and neutral lipids were shown to reduce the aggregation propensity of αSyn by inducing its folding into an α-helix.[17] This effect of membranes strongly depends on the charge of polar groups, saturation of aliphatic tails, membrane curvature, and lipid-to-protein ratio.[18] The reported contradictions can be explained by changes in the fibril morphology due to coaggregation with lipids.[19] A majority of the studies of the membranes influence on αSyn aggregation was performed when the mechanism of αSyn fibrillization was not yet well understood. Namely, effect of lipids on *de novo* fibril formation and fibril growth was not considered independently.

In this work, we took into account the latest knowledge on the mechanism of αSyn fibrillization to separately investigate the influence of membranes on the lag phase and the fibril elongation phase. Based on our results, we proposed a model that explains the strong effect of membranes on fibrillization.

To study the influence of membrane binding on αSyn fibrillization, we used small unilamellar vesicles (SUVs) and

Received: December 24, 2020
Accepted: February 4, 2021
Published: February 10, 2021

monitored the amount of formed fibrils using Thioflavin T (ThT), a dye that strongly increases its fluorescence intensity upon binding to amyloid fibrils and is almost not sensitive to the presence of membranes (Figure S5).

Electrostatic interactions have a major impact on αSyn binding to the lipid membranes. Therefore, we started our studies with comparing the effects of lipid membranes of different charge on αSyn fibrillization. We incubated αSyn in the presence of SUVs composed of neutral palmitoyl-oleoyl-phosphatidylcholine (POPC) and anionic palmitoyl-oleoyl-phosphoglycerol (POPG) lipids. Membranes led to an ∼5-fold decrease in the amount of fibrils formed during 75 h (Figure 1A), and the effect did not significantly depend on the membrane charge. We chose membranes composed of a POPC/POPG 3:1 mixture, as their net charge is close to that of the inner leaflet of cell plasma membranes.[20]

To clarify if membranes influence the fibril elongation process or early stages of αSyn aggregation, we performed experiments that allow one to study their kinetics separately. αSyn aggregation is characterized by a relatively long lag phase followed by a fast exponential growth of the fibrillized protein fraction. The time until the beginning of the exponential growth depends on the rate of early stages of the aggregation including multistep formation of initial fibrils from αSyn monomers. After slow formation of the first fibrils, they are rapidly multiplied via an autocatalytic mechanism[21] that leads to high sample-to-sample variability of the time until the beginning of the exponential growth phase. To quantify this process, we measured the time necessary for fibrillization of the first 2% of αSyn, which is the minimal amount that can be clearly detected in light-scattering of the lipid solutions. Without lipids, the exponential growth starts at ∼33 h, while addition of the membranes increased this time to >120 h already at 16 lipids/αSyn (Figure 1B).

Already at 1:1 lipid/αSyn ratio, the lag phase increases almost twice, while a higher concentration of the membranes led to even stronger slowdown (Figure 1C). A significant fraction of the samples with the lipid/αSyn ratios of 8−16 did not start the exponential fibril growth even during 5 days (Figure S1).

αSyn binds to the membrane as an α-helix oriented parallel to the membrane surface,[22] and the binding stoichiometry is limited by its size. To determine the affinity and stoichiometry of the interaction, we titrated αSyn with lipid membranes following the interaction by the circular dichroism (CD) signal at 225 nm (Figure 2E). Less than 4% of αSyn was bound to POPC:POPG (3:1) at a lipid/αSyn ratio of 1:1 (Figure 1C, right scale). Such a minor decrease in the concentration of free monomeric αSyn cannot lead to the observed 2-fold drop in the rate of initial fibrils formation. Therefore, the increase in $t_{2\%}$ is caused by membrane binding of the species present at much lower concentrations than that for the monomeric protein. We observed a delay of the exponential fibrillization phase in the presence of fluid membranes of moderate charge, in accordance with previously reported suppression of overall αSyn fibrillization by such membranes.[23] Meanwhile, for membranes composed only of anionic lipids, an opposite effect was reported[16] (Table S1). Indeed, rigid membranes composed of saturated anionic lipids DPPG did not slow down the fibrillization (Figure S3). Fluid anionic POPG membranes slow down the fibrillization initiation less than membranes composed of a POPC/POPG mixture (Figure S4). Likely, the ability of membranes to sequester prefibrillar species depends not only on the affinity but also on selectivity, that is lower in the case of anionic membranes that bind monomeric αSyn with high affinity.[24]

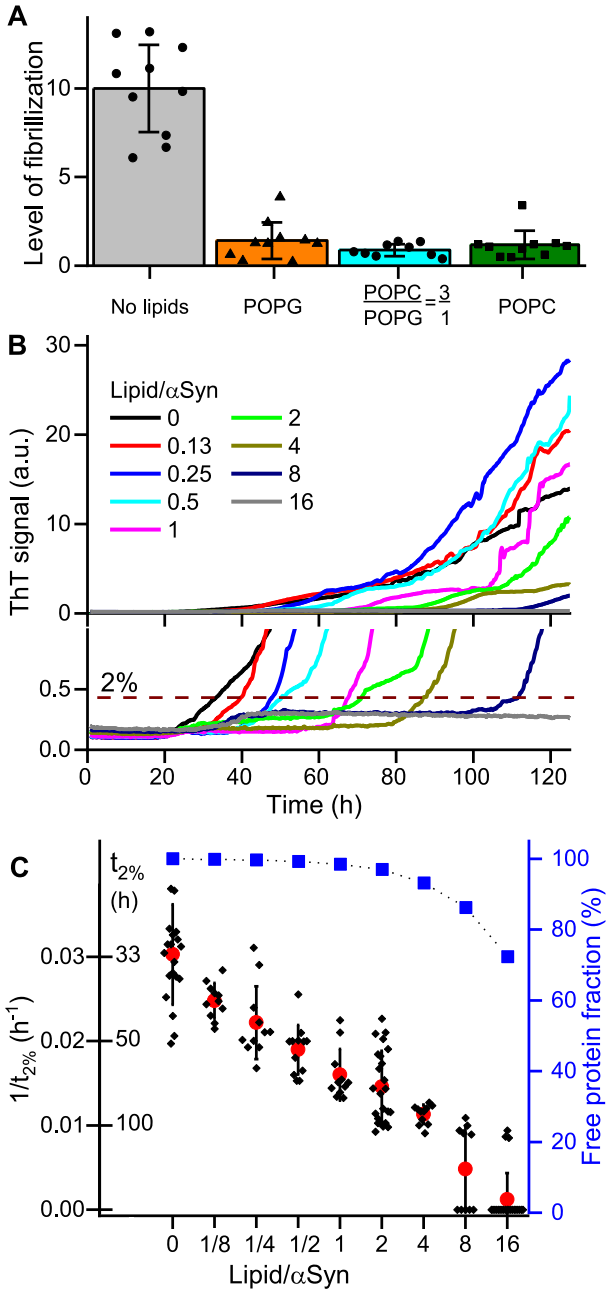

Figure 1. Influence of lipid membranes on αSyn fibrillization. (A) Amount of fibrillized αSyn formed from 50 μM monomer after 75 h incubation, as quantified by ThT fluorescence, no lipids, and 10 lipids/αSyn. (B) αSyn fibrillization in the presence and absence of lipid membranes (SUVs, 3:1 POPC/POPG mixture). Median kinetic curves of 12−24 measurements (see Figure S1 for all traces). (C) Delay of the exponential phase of αSyn fibrillization at different lipid/αSyn ratios, calculated as reciprocal of time to reach 2% fibrillization (see panel B). Whiskers are SD 100 μM αSyn and 0 to 1600 μM lipids. 12−24 repeats. Blue squares show the fraction of free protein (right scale) calculated using eq 2 and K_d = 87 nM and n = 230 lipid/αSyn.

To measure the fibril elongation rate independently from the primary nucleation, we initiated αSyn fibrillization by addition of short sonicated preformed fibrils (so-called "seeds") to αSyn

https://dx.doi.org/10.1021/acschemneuro.0c00819
ACS Chem. Neurosci. 2021, 12, 825−830

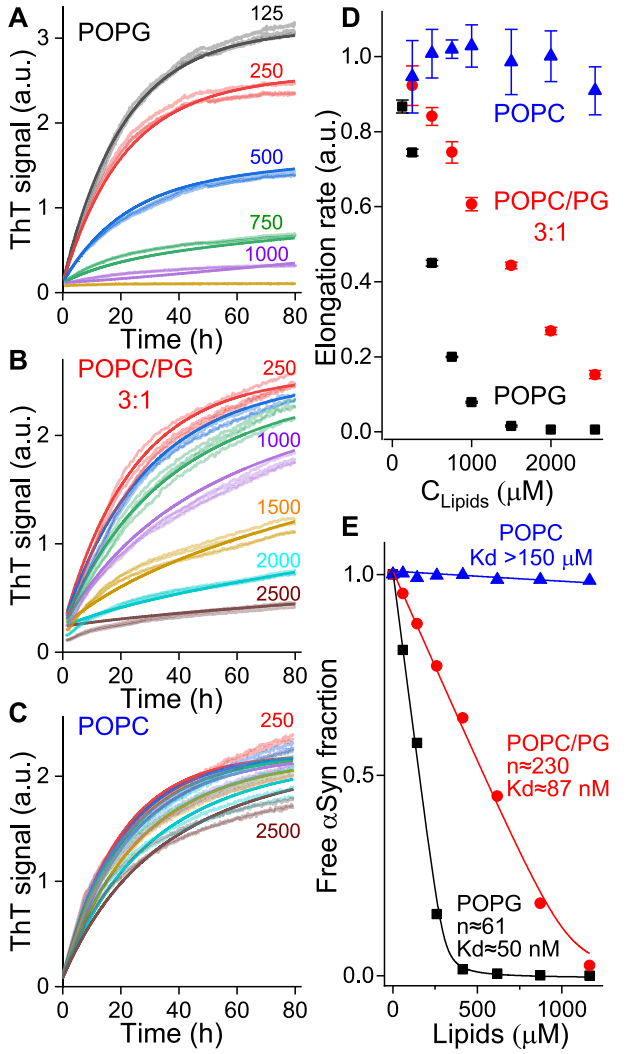

Figure 2. Influence of lipid membranes on the fibril growth rate. (A–C) Kinetics of seeded αSyn fibrillization at 125–2500 μM lipid concentrations. Four repeats per concentration and global fit for each lipid composition. SUVs composed of POPG (A), POPC/POPG 3:1(B), and POPC (C). αSyn and seed concentrations were 25 and 0.5 μM, respectively. (D) Initial αSyn fibril elongation rate as a function of lipid concentration. Averages from traces presented in panels (A)–(C). Error bars are SD. (E) Fraction of free αSyn as a function of lipid concentration calculated based on CD spectra. Stoichiometry (n) and dissociation constant (K_d) were determined by fitting (see Figure S11 for details). Concentration of αSyn was 5 μM.

solution. These seeds provided many centers for fibril elongation making the influence of primary nucleation process negligible.[21]

The presence of membranes induced slowdown of αSyn fibril elongation, and decreased the amount of formed fibrils (Figure 2A–C). The effect was strongest in the case of anionic POPG that tightly binds αSyn. It almost blocked the fibril formation already at 60:1 lipid-to-protein ratio (Figure 2A). On the other hand, neutral POPC membranes that have low affinity to αSyn induced only moderate changes (Figure 2C). The fibrillization rates calculated from kinetic curves (Figure 2D) decrease with the lipid concentration in the same way as the fraction of free protein determined by circular dichroism titration (Figure 2E). A similar decrease of fibrillization rate was observed also in the presence of rigid DPPG membranes (Figure S10). We hypothesize that the fibrillization rate is proportional to the concentration of nonbound αSyn monomer while the membrane-bound αSyn does not participate in the fibril formation. This hypothesis is supported by experiments with excess of αSyn over lipids in which all membranes are saturated with the protein and lipid-induced decrease of the fibril growth rate is linearly proportional to the lipid concentration (Figure S9).

We developed a simple mathematical model that describes the kinetics of αSyn fibril growth in the presence of membranes based on this hypothesis. αSyn binding to membrane occurs on the millisecond scale[24] and can be considered instant compared to its interaction with fibrils. Therefore, the rate of fibril growth is determined mostly by the binding of free monomer to the fibril end. Under seeded conditions, the concentration of fibril ends can be considered constant, and the evolution of the fraction of fibrillized protein with time can be expressed by

$$f = 1 - \alpha \exp(-tkC_{ends}) - (1 - \alpha) \exp(-tkC_{ends}Kd/C_p) \quad (1)$$

where f is the fraction of fibrillized αSyn at time t, k is the rate constant of monomer binding to the fibril end, C_{ends} is the concentration of fibril ends, α is the fraction of free protein calculated based on its K_d to the membrane according to eq 2, and C_p is the initial monomer concentration. The term $\alpha \exp(-tkC_{ends})$ corresponds to the fast fibrillization of the free protein, while the term $(1 - \alpha) \exp(-tkC_{ends}K_d/[M]_0)$ describes slow fibrillization of the residual monomer that occurs after its dissociation from membrane (see SI section 4 for a more detailed explanation). We used this equation to do a global fit of the kinetic curves of αSyn fibrillization in the presence of different lipid concentrations. It properly describes the observed decrease of the fibril elongation rate and the amount of fibrillized protein (plateau value) in the presence of lipids (Figure 2A–C). The affinities of αSyn to membrane and lipid:protein stoichiometries obtained from fitting of kinetic curves (Figure S8) show the same dependence on membrane charge as ones obtained in independent steady state titration experiments (Figure 2E).

To prove that lipid-bound αSyn remains nonfibrillized even when the fibrillization reaches equilibrium plateau, we used αSyn labeled with an environmentally sensitive dye 7AFM (Figure 3), a fluorophore that can distinguish between disordered, fibrillized, and membrane-bound forms of the labeled protein by the shape of its two-band emission spectrum[25] (Figure S12).

We mixed αSyn with 4% αSyn-18C labeled with 7AFM and compared the emission spectra of the label at the final and initial points of the aggregation. In the absence of membranes, spectra of 7AFM showed a transition of completely monomeric αSyn to the fibrillar form (Figure 3B, black curves). With the lipid vesicles, the fluorescence spectrum at the initial point was different from the spectrum of free monomer showing a binding of ~65% of αSyn to the membrane (intense band at ~590 nm). The fibrillization of membrane-containing sample reached a plateau in 30 h, and the intensity of its ThT signal was ~3-fold lower than that without membrane (Figure 3A). The spectrum of 7AFM label for this fibrillized sample shows a strong characteristic band at ~590 nm indicating that a significant part of labeled protein is still membrane-bound (Figure 3B, solid red curve). The spectrum was equal to the linear combination of the spectra of membrane-bound αSyn monomer (~65%) and of fibrillized

https://dx.doi.org/10.1021/acschemneuro.0c00819
ACS Chem. Neurosci. 2021, 12, 825–830

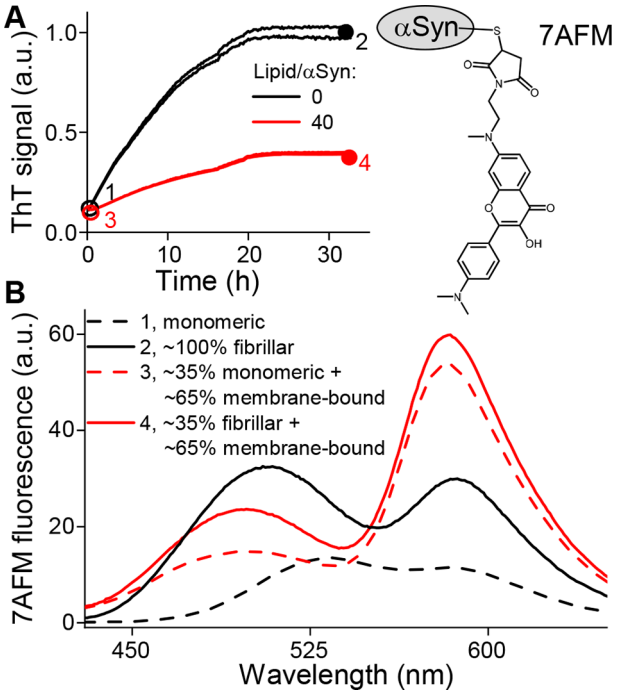

Figure 3. Part of αSyn remains nonfibrillized in the presence of membranes. (A) Fibrillization of αSyn in the absence (black) and in the presence (red) of 750 μM lipids (SUVs, 1:3 POPC/POPG mixture). 25 μM αSyn, 4% was labeled by 7AFM dye. Seeds concentration was 500 nM. (B) Fluorescence spectra of 7AFM at initial (dashed lines) and final (solid lines) stages of αSyn fibrillization, at time points marked in panel (A).

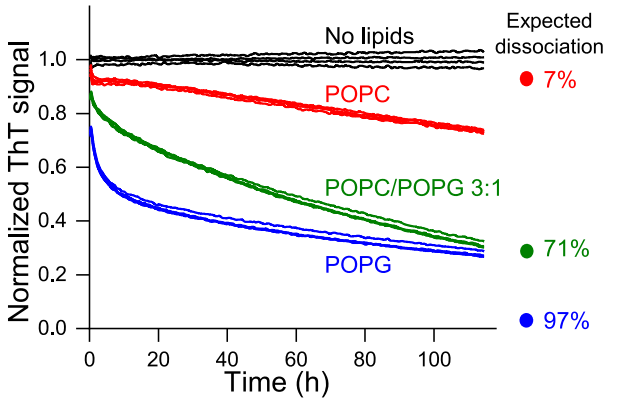

Figure 4. Dissociation of 10 μM αSyn fibrils into monomers in the presence of 1600 μM lipids. Normalized traces with no lipids (black), POPC (red), POPC/POPG 3:1 (green), and POPG (blue) liposomes. Dots represent expected final values calculated based on αSyn affinity to corresponding lipids.

αSyn (~35%), in agreement with the intensity of ThT fluorescence (Figures 3A and S12).

Taken together, our data demonstrate that elongation of amyloid fibrils occurs only in the presence of free monomeric αSyn in solution.

The monomeric αSyn in solution is in equilibrium with membrane-bound protein, and its concentration is determined by the affinity to the membranes. In the case of anionic membranes, the interaction is quite strong (K_d per binding site is about 50 nM).[26] Therefore, the equilibrium concentration of free monomeric protein in the presence of anionic membranes is much lower than the minimal concentration required for fibril growth (~400 nM[27]). To prove that binding of αSyn to the fibril end or to the membrane is an equilibrium process, we incubated short αSyn fibrils in the presence of excess of lipid vesicles (1600 μM lipids and 10 μM αSyn). The observed disaggregation of short αSyn fibrils (Figure 4) clearly shows that the fibrillization is reversible and that the affinity of the αSyn monomer to the fibril end is lower than its affinity to the membranes. This finding is in agreement with the previously reported dissociation of αSyn fibrils in the presence of DMPS SUVs.[16]

Our findings are in a good agreement with numerous reports of slowdown of αSyn aggregation in the presence of high concentrations of lipid membranes.[17,18,23,28] The low fibrillization propensity of membrane-bound αSyn can be explained by thermodynamic factors. Membrane-bound αSyn is stabilized in the helical form by tens of intramolecular hydrogen bonds and strong hydrophobic interactions with the membrane. Its conversion to amyloid form is less energetically favored than conversion of unstructured monomer containing only few intramolecular hydrogen bonds.

To sum up, we found that membrane-bound monomeric αSyn does not participate in the fibril elongation process. Moreover, excess of membranes with high affinity to αSyn induces disaggregation of already formed fibrils (Figure 5).

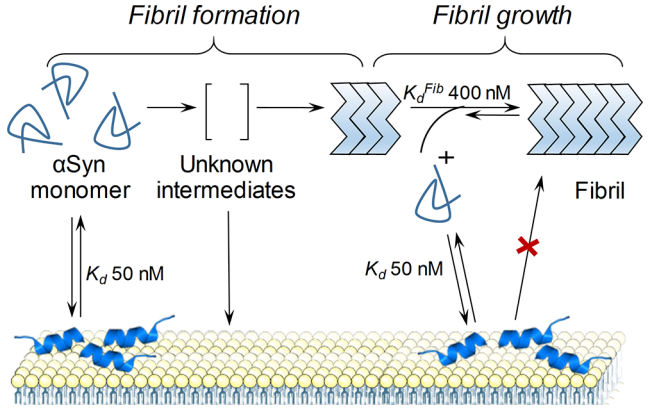

Figure 5. Scheme of αSyn fibrillization in the presence of lipid membranes. A fraction of monomeric αSyn accumulates on the lipid membranes and cannot proceed to fibrillization, because its affinity to anionic membranes (K_d ~ 50 nM) is higher than that to fibril ends (K_d^{Fib} ~ 400 nM).

The beginning of the exponential growth of αSyn fibrils is delayed even by a small amount of lipids. Therefore, membranes make crucial impact on the rate and equilibrium of αSyn fibrillization. We believe that these findings help to better understand the role of membranes in the interconversion between physiological and fibrillized forms of αSyn during Parkinson's disease.

METHODS

Preparation of Recombinant αSyn. Plasmids (pT7-7 vector) encoding αSyn or αSyn-A18C were kindly provided by the group of Vinod Subramaniam, University of Twente. The proteins were expressed in *E. coli* and purified by ion exchange FPLC as described earlier.[29] Prior to use, protein solutions were centrifuged at 14 000*g* for 30 min to remove possible aggregates. The concentration was measured by tyrosine absorbance using ε_{275} = 6000 M^{-1} cm^{-1}. For the

https://dx.doi.org/10.1021/acschemneuro.0c00819
ACS Chem. Neurosci. 2021, 12, 825−830

detailed protocol and protein sequences, see the Supporting Information.

Liposome Preparation. All lipids were purchased from Avanti Polar Lipids. Solutions of lipid mixtures in $CHCl_3$ were dried and lipids were hydrated with buffer solution for kinetic measurements (Na/PO_4 6 mM pH 7.4, NaCl 150 mM, NaN_3 10 mM, EDTA 0.1 mM, and ThT 5 μM) and sonicated to prepare SUVs (Figure S13) as described earlier.[25]

Kinetic Experiments. The kinetics of αSyn fibrillization was measured *in situ* using a Tecan SPARK plate reader at 37 °C. The fluorescence intensity of ThT (proportional to the fibrillized protein fraction) was measured every 300 s. The plate was left quiescent except for 5 s shaking (90 rpm) prior each measurement. Excitation and emission wavelengths were 441 nm (slit 5 nm) and 480 nm (slit 8−20 nm), respectively. The experiments were performed in a black 384-well plate with a transparent bottom (cat. no. 242764; Nunc/Thermo Fisher Scientific) covered with plastic film ("Viewseal", Greiner Bio One) to prevent evaporation. The fluorescence was recorded from the bottom of the plate. Each well contained 50 μL of a sample solution. The buffer composition: 6 mM Na/PO_4 buffer pH 7.4, 150 mM NaCl, 10 mM NaN_3, 0.1 mM EDTA and 5 μM ThT.

Kinetics of Nonseeded Aggregation. Stock solutions of αSyn and lipid vesicles were mixed with buffer to yield 700 μL of solution, containing 100 μM αSyn and desirable concentration of lipids. The solution was pipetted in 12 wells (50 μL/well) and the fibrillization kinetics was monitored during ∼5 days. The time needed for 2% protein fibrillization ($t_{2\%}$) was calculated based on the ThT signal (Figure 1B).

Preparation of Seeds. We initiated αSyn fibrillization by adding short fibrils (seeds) to the solution of monomeric protein. The seeds were prepared by sonication of mature αSyn fibrils (sample of αSyn that reached the fibrillization plateau according to ThT fluorescence). A microcentrifuge tube with 50 μL of fibril solution was immersed in a low power bath sonicator (Digitec DT 100, Sonorex, Germany) for 15 min. This procedure yielded the fibrils with average length of ∼50 nm.[29]

Measurements of the Fibril Elongation Rate. Monomeric αSyn (25 μM) was mixed with 0.25−0.5 μM seeds (1−2% of used monomer concentration). The solution was resuspended and immediately mixed with liposomes solution (up to 2.5 mM final lipid concentration). This procedure ensures equal seed distribution between the samples. After that we pipetted the final solutions into the plate (4−6 repeats for each lipid concentration) and measured the ThT fluorescence intensity as a function of time for 80 h. The experiment was repeated three times. The fibril elongation rate was calculated based on the increase of ThT signal at the initial part of a kinetic curve (between 1200 and 9000 s), during which the rate was almost constant. The relative reaction rate (R/R_0) is the ratio of fibril growth in the absence and in the presence of lipids.

Affinity of αSyn to Membranes. The affinity of αSyn to the membranes was calculated based on circular dichroism (CD) titration data. CD spectra were recorded with a JASCO-J810 spectropolarimeter. Samples of 5 μM αSyn were titrated with corresponding lipid solutions. The spectra were recorded using a 2 mm path length cuvette at room temperature, scanning from 200 to 250 nm with a step size of 0.1 nm and a scanning speed of 50 nm/min. The signal/noise ratio was improved by accumulating and averaging of three scans. All spectra were corrected by subtracting the background spectrum of the buffer.

The CD signal at 225 nm is approximately proportional to α-helix content. To convert it to the fraction of membrane-bound protein we normalized it to the plateau value for POPG titration where the complete binding was reached.

The results were fitted with the following equation:

$$\alpha = \frac{K_d + C_p + C_L/n - \sqrt{(K_d + C_p + C_L/n)^2 - 4C_pC_L/n}}{2C_p} \quad (2)$$

where α is the fraction of membrane-bound protein, C_p is the protein concentration, C_L is the concentration of lipids, n is the number of lipids per binding site, and K_d is the dissociation constant. K_d and n values were optimized to obtain the best fit.

Aggregation Assessment by Environmentally Sensitive Dye. αSyn-18C-7AFM was prepared by labeling the αSyn-18C mutant with a maleimide derivative of 7AFM.[25] The unreacted label was removed by two filtrations through a 7k MWCO Zeba Spin column (Thermo Fisher Scientific). The concentration of the labeled protein was determined by absorbance, ε_{405} = 35 000 M^{-1} cm^{-1} for 7AFM (see the Supporting Information for the detailed labeling protocol).

We mixed 24 μM αSyn and 1 μM αSyn-18C-7AFM and monitored the fibrillization by fluorescence of environment-sensitive dye 7AFM.[25] A volume of 600 μL of αSyn solution in the presence and absence of lipid membranes (1 mM POPC/POPG = 3:1, 40 lipids/αSyn) was prepared in the same buffer as for kinetic measurements but without ThT. The fibrillization was initiated by addition of 2% of seeds, and 10 parallel repeats were pipetted to different wells (50 μL/well). Two repeats containing ThT were pipetted to the same plate. The fibrillization was performed in plate reader as described above. After 35 h, the ThT fluorescence intensity reached the plateau. ThT-free repeats of each sample were combined and used for fluorescence spectroscopy measurements. The experiment was repeated twice using different batches of αSyn and lipids.

The emission spectra of 7AFM were recorded on Fluoromax 4 spectrofluorometer in a 2 mm path length quartz cuvette. All spectra were recorded at room temperature and corrected for baseline light scattering. The excitation wavelength was 390 nm (3 nm slits). The amount of membrane-bound and fibrillized αSyn was calculated by deconvoluting the emission spectra as a linear combination of spectra of pure free, membrane-bound, and completely fibrillized samples measured independently.[25]

■ ASSOCIATED CONTENT

Supporting Information

The Supporting Information is available free of charge at https://pubs.acs.org/doi/10.1021/acschemneuro.0c00819.

Additional kinetic curves. Response of ThT fluorescence on lipids; literature overview on influence of lipids on αSyn aggregation; details of mathematical model; rates of fibril growth at low amounts of lipid membranes; fluorescence spectra of αSyn-7AFM; protocols for protein preparation and labeling, liposomes preparation protocols; TEM images of αSyn fibrils (PDF)

■ AUTHOR INFORMATION

Corresponding Author

Volodymyr V. Shvadchak − *Czech Academy of Sciences, Institute of Organic Chemistry and Biochemistry, Prague 166 10, Czech Republic;* orcid.org/0000-0001-8302-8073; Email: shvadchak@gmail.com

Authors

Andrii S. Kurochka − *Czech Academy of Sciences, Institute of Organic Chemistry and Biochemistry, Prague 166 10, Czech Republic; Department of Analytical Chemistry, University of Chemistry and Technology, Prague 166 28, Czech Republic;* orcid.org/0000-0001-9986-3559

Dmytro A. Yushchenko − *Czech Academy of Sciences, Institute of Organic Chemistry and Biochemistry, Prague 166 10, Czech Republic; Miltenyi Biotec GmbH, Bergisch Gladbach 51429, Germany;* orcid.org/0000-0003-0355-6197

Petr Bouř − *Czech Academy of Sciences, Institute of Organic Chemistry and Biochemistry, Prague 166 10, Czech Republic;*

https://dx.doi.org/10.1021/acschemneuro.0c00819
ACS Chem. Neurosci. 2021, 12, 825−830

Department of Analytical Chemistry, University of Chemistry and Technology, Prague 166 28, Czech Republic;
orcid.org/0000-0001-8469-1686

Complete contact information is available at:
https://pubs.acs.org/10.1021/acschemneuro.0c00819

Author Contributions

D.A.Y. and V.V.S. designed the research, A.S.K. carried out the experiments, A.S.K. and V.V.S. analyzed the results, and all authors participated in writing the manuscript.

Funding

This work was supported by Czech Science Foundation [GAČR Grants 18-06255Y and 20-10144S] and Ministry of Education [CZ.02.1.01/0.0/0.0/16_019/0000729].

Notes

The authors declare no competing financial interest.

REFERENCES

(1) Iwai, A., Masliah, E., Yoshimoto, M., Ge, N., Flanagan, L., de Silva, H. A., Kittel, A., and Saitoh, T. (1995) The precursor protein of non-A beta component of Alzheimer's disease amyloid is a presynaptic protein of the central nervous system. *Neuron 14* (2), 467−475.

(2) Auluck, P. K., Caraveo, G., and Lindquist, S. (2010) α-Synuclein: membrane interactions and toxicity in Parkinson's disease. *Annu. Rev. Cell Dev. Biol. 26*, 211−233.

(3) Murphy, D. D., Rueter, S. M., Trojanowski, J. Q., and Lee, V. M. (2000) Synucleins are developmentally expressed, and α-synuclein regulates the size of the presynaptic vesicular pool in primary hippocampal neurons. *J. Neurosci. 20* (9), 3214−3220.

(4) Jao, C. C., Hegde, B. G., Chen, J., Haworth, I. S., and Langen, R. (2008) Structure of membrane-bound α-synuclein from site-directed spin labeling and computational refinement. *Proc. Natl. Acad. Sci. U. S. A. 105* (50), 19666−19671.

(5) Goedert, M., Spillantini, M. G., Del Tredici, K., and Braak, H. (2013) 100 years of Lewy pathology. *Nat. Rev. Neurol. 9* (1), 13−24.

(6) Li, B., Ge, P., Murray, K. A., Sheth, P., Zhang, M., Nair, G., Sawaya, M. R., Shin, W. S., Boyer, D. R., Ye, S., Eisenberg, D. S., Zhou, Z. H., and Jiang, L. (2018) Cryo-EM of full-length α-synuclein reveals fibril polymorphs with a common structural kernel. *Nat. Commun. 9* (1), 3609.

(7) Zhang, X. L., Wesen, E., Kumar, R., Bernson, D., Gallud, A., Paul, A., Wittung-Stafshede, P., and Esbjorner, E. K. (2020) Correlation between Cellular Uptake and Cytotoxicity of Fragmented α-Synuclein Amyloid Fibrils Suggests Intracellular Basis for Toxicity. *ACS Chem. Neurosci. 11* (3), 233−241.

(8) Peelaerts, W., Bousset, L., Van der Perren, A., Moskalyuk, A., Pulizzi, R., Giugliano, M., Van den Haute, C., Melki, R., and Baekelandt, V. (2015) α-Synuclein strains cause distinct synucleinopathies after local and systemic administration. *Nature 522* (7556), 340−344.

(9) Burre, J., Sharma, M., and Sudhof, T. C. (2015) Definition of a molecular pathway mediating α-synuclein neurotoxicity. *J. Neurosci. 35* (13), 5221−5232.

(10) Polymeropoulos, M. H., Lavedan, C., Leroy, E., Ide, S. E., Dehejia, A., Dutra, A., Pike, B., Root, H., Rubenstein, J., Boyer, R., Stenroos, E. S., Chandrasekharappa, S., Athanassiadou, A., Papapetropoulos, T., Johnson, W. G., Lazzarini, A. M., Duvoisin, R. C., Di Iorio, G., Golbe, L. I., and Nussbaum, R. L. (1997) Mutation in the α-synuclein gene identified in families with Parkinson's disease. *Science 276* (5321), 2045−2047.

(11) Ruf, V. C., Nubling, G. S., Willikens, S., Shi, S., Schmidt, F., Levin, J., Botzel, K., Kamp, F., and Giese, A. (2019) Different Effects of α-Synuclein Mutants on Lipid Binding and Aggregation Detected by Single Molecule Fluorescence Spectroscopy and ThT Fluorescence-Based Measurements. *ACS Chem. Neurosci. 10* (3), 1649−1659.

(12) Arosio, P., Knowles, T. P., and Linse, S. (2015) On the lag phase in amyloid fibril formation. *Phys. Chem. Chem. Phys. 17* (12), 7606−7618.

(13) Volles, M. J., and Lansbury, P. T., Jr. (2003) Zeroing in on the pathogenic form of α-synuclein and its mechanism of neurotoxicity in Parkinson's disease. *Biochemistry 42* (26), 7871−7878.

(14) Gaspar, R., Meisl, G., Buell, A. K., Young, L., Kaminski, C. F., Knowles, T. P. J., Sparr, E., and Linse, S. (2017) Secondary nucleation of monomers on fibril surface dominates α-synuclein aggregation and provides autocatalytic amyloid amplification. *Q. Rev. Biophys. 50*, No. e6.

(15) Galvagnion, C. (2017) The Role of Lipids Interacting with α-Synuclein in the Pathogenesis of Parkinson's Disease. *J. Parkinson's Dis. 7* (3), 433−450.

(16) Galvagnion, C., Buell, A. K., Meisl, G., Michaels, T. C., Vendruscolo, M., Knowles, T. P., and Dobson, C. M. (2015) Lipid vesicles trigger α-synuclein aggregation by stimulating primary nucleation. *Nat. Chem. Biol. 11* (3), 229−234.

(17) Zhu, M., Li, J., and Fink, A. L. (2003) The association of α-synuclein with membranes affects bilayer structure, stability, and fibril formation. *J. Biol. Chem. 278* (41), 40186−40197.

(18) Rocha, S., Kumar, R., Horvath, I., and Wittung-Stafshede, P. (2019) Synaptic vesicle mimics affect the aggregation of wild-type and A53T α-synuclein variants differently albeit similar membrane affinity. *Protein Eng., Des. Sel. 32* (2), 59−66.

(19) Hellstrand, E., Nowacka, A., Topgaard, D., Linse, S., and Sparr, E. (2013) Membrane lipid co-aggregation with α-synuclein fibrils. *PLoS One 8* (10), No. e77235.

(20) Ingolfsson, H. I., Melo, M. N., van Eerden, F. J., Arnarez, C., Lopez, C. A., Wassenaar, T. A., Periole, X., de Vries, A. H., Tieleman, D. P., and Marrink, S. J. (2014) Lipid organization of the plasma membrane. *J. Am. Chem. Soc. 136* (41), 14554−14559.

(21) Buell, A. K., Galvagnion, C., Gaspar, R., Sparr, E., Vendruscolo, M., Knowles, T. P., Linse, S., and Dobson, C. M. (2014) Solution conditions determine the relative importance of nucleation and growth processes in alpha-synuclein aggregation. *Proc. Natl. Acad. Sci. U. S. A. 111* (21), 7671−7676.

(22) Hellstrand, E., Grey, M., Ainalem, M. L., Ankner, J., Forsyth, V. T., Fragneto, G., Haertlein, M., Dauvergne, M. T., Nilsson, H., Brundin, P., Linse, S., Nylander, T., and Sparr, E. (2013) Adsorption of α-Synuclein to Supported Lipid Bilayers: Positioning and Role of Electrostatics. *ACS Chem. Neurosci. 4* (10), 1339−1351.

(23) Grey, M., Dunning, C. J., Gaspar, R., Grey, C., Brundin, P., Sparr, E., and Linse, S. (2015) Acceleration of α-synuclein aggregation by exosomes. *J. Biol. Chem. 290* (5), 2969−2982.

(24) Shvadchak, V. V., Falomir-Lockhart, L. J., Yushchenko, D. A., and Jovin, T. M. (2011) Specificity and kinetics of α-synuclein binding to model membranes determined with fluorescent excited state intramolecular proton transfer (ESIPT) probe. *J. Biol. Chem. 286* (15), 13023−13032.

(25) Kucherak, O. A., Shvadchak, V. V., Kyriukha, Y. A., and Yushchenko, D. A. (2018) Synthesis of a Fluorescent Probe for Sensing Multiple Protein States. *Eur. J. Org. Chem. 2018*, 5155−5162.

(26) Shvadchak, V. V., Kucherak, O., Afitska, K., Dziuba, D., and Yushchenko, D. A. (2017) Environmentally sensitive probes for monitoring protein-membrane interactions at nanomolar concentrations. *Biochim. Biophys. Acta, Biomembr. 1859* (5), 852−859.

(27) Agerschou, E. D., Flagmeier, P., Saridaki, T., Galvagnion, C., Komnig, D., Heid, L., Prasad, V., Shaykhalishahi, H., Willbold, D., Dobson, C. M., Voigt, A., Falkenburger, B., Hoyer, W., and Buell, A. K. (2019) An engineered monomer binding-protein for α-synuclein efficiently inhibits the proliferation of amyloid fibrils. *eLife 8*, e46112.

(28) Zhu, M., and Fink, A. L. (2003) Lipid binding inhibits α-synuclein fibril formation. *J. Biol. Chem. 278* (19), 16873−16877.

(29) Afitska, K., Fucikova, A., Shvadchak, V. V., and Yushchenko, D. A. (2019) α-Synuclein aggregation at low concentrations. *Biochim. Biophys. Acta, Proteins Proteomics 1867* (7−8), 701−709.